Hyperfine Interact
DOI 10.1007/s10751-012-0707-3

Critical behaviour of $Ho_2Fe_{17-x}Mn_x$—magnetisation and Mössbauer spectroscopy

J. L. Wang · S. J. Campbell · S. J. Kennedy · S. X. Dou

© Springer Science+Business Media Dordrecht 2012

Abstract The magnetic properties of $Ho_2Fe_{17-x}Mn_x$ compounds (x = 0–2) of ferromagnetic ordering temperatures up to $T_C \sim 344$ K have been investigated by DC magnetization and Mössbauer effect measurements. The nature of the magnetic phase transitions and the critical behaviour around T_C has been investigated by analysis of the magnetisation data and the critical exponents β, γ and δ determined. The critical exponents are found to be similar to the theoretical values of the mean-field model for which $\beta = 0.5$ and $\gamma = 1.0$, indicating the existence of a long-range ferromagnetic interactions. The isothermal entropy changes ΔS around T_C have been determined as a function of temperature in different magnetic fields.

Keywords Magnetisation · Mössbauer spectroscopy · Critical exponents · Magnetocaloric · $Ho_2Fe_{17-x}Mn_x$

1 Introduction

Magnetic refrigeration based on the magnetocaloric effect (MCE) has attracted increasing attention in recent years due to advantages such as high efficiency and environmental safety compared with compressor-based refrigeration [e.g. 1, 2]. Considering scientific aspects and industrial applicability, the large gJ value in iron

J. L. Wang · S. X. Dou
Institute for Superconductivity and Electronic Materials, University of Wollongong, Wollongong, NSW 2522, Australia

J. L. Wang · S. J. Kennedy
Bragg Institute, ANSTO, Menai, NSW 2234, Australia

J. L. Wang · S. J. Campbell (✉)
School of Physical, Environmental and Mathematical Sciences, The University of New South Wales, Canberra, ACT 2600, Australia
e-mail: stewart.campbell@adfa.edu.au

Published online: 20 November 2012

and the low cost of iron means that Fe-rich materials offer a potential choice as MCE materials for refrigerators [3, 4] and as a result, materials such as R_2Fe_{17}-based compounds have continued to attracted interest [5].

Recently we reported [6, 7] that the substitution of Mn for Fe in $Ho_2Fe_{17-x}Mn_x$ compounds leads to a minimum of M_s at 10 K and a maximum of T_C in the composition dependence of M_s (at T = 10 K) and T_C as well as the presence of strong magnetovolume effects below T_C. In order to better understand the nature of the magnetic phase transition around T_C in these systems, we have carried out a detailed investigation of the critical behaviour by DC magnetization measurements and Mössbauer spectroscopy with the main findings reported here.

2 Experimental

The $Ho_2Fe_{17-x}Mn_x$ compounds (x = 0, 0.5, 1, 2) were prepared by standard argon arc-melting (see [5–7] for details). The magnetic measurements were carried out in magnetic fields up to 6 T over the temperature range 5–350 K using a Physical Property Measurement System [6, 7]. ^{57}Fe Mössbauer spectra were obtained using a standard constant-acceleration spectrometer and a ^{57}CoRh source and the spectrometer calibrated at room temperature with an α-iron foil.

3 Results and discussion

3.1 Mössbauer spectroscopy

Figure 1a shows the ^{57}Fe Mössbauer spectra at 300 K for $Ho_2Fe_{17-x}Mn_x$ (x = 0, 0.5 and 1.0). Given that the Curie temperatures for the x = 0, 0.5 and 1.0 samples are above room temperature—T_C = 336 K, T_C = 344 K and T_C = 338 K respectively [7]—the 300 K spectra are found to exhibit spectral features characteristic of magnetic hyperfine splitting as expected. We have fitted the $Ho_2Fe_{17-x}Mn_x$ spectra using the same approach applied to our analysis of $Dy_2Fe_{17-x}Mn_x$ ([5], see also [6]). As shown by Fig. 1a, satisfactory fits to the Mössbauer spectra were obtained using seven sub-spectra to represent the four inequivalent sites of the Th_2Ni_{17}-type structure (or the Th_2Zn_{17} structure in brackets)—one sub-spectrum for the 4f (6c) site, two for 6g (9d), two for 12 j (18f) and two for 12k (18h). The sub-spectra were assigned to the various sites by taking into account the nearest-neighbour environment of each respective site and the Fe-Fe distances [5].

The main hyperfine parameters at 300 K are listed in Table 1. It can be seen that the isomer shifts follow the trends $\delta^{4f(6c)} > \delta^{12j(18f)} > \delta^{12k(18h)} > \delta^{6g(9d)}$ for all compounds. The calculated Wigner-Seitz cell (WSC) volumes V_{ws} for the 4f (6c), 6g (9d), 12j (18f) and 12k (18h) sites in R_2Fe_{17} compounds have been shown to behave as follows: $V_{ws}{}^{4f(6c)} > V_{ws}{}^{12j(18f)} > V_{ws}{}^{12k(18h)} > V_{ws}{}^{6g(9d)}$ [5, 8]. The present findings agree well with the previously observed relationship between isomer shift and WSC volumes, namely that the larger the WSC volume, the larger the isomer shift δ [5, 6].

The temperature dependences of the ^{57}Fe hyperfine interaction parameters for $Ho_2Fe_{16.5}Mn_{0.5}$ are shown in Fig. 1b as a typical example of the behaviour of these

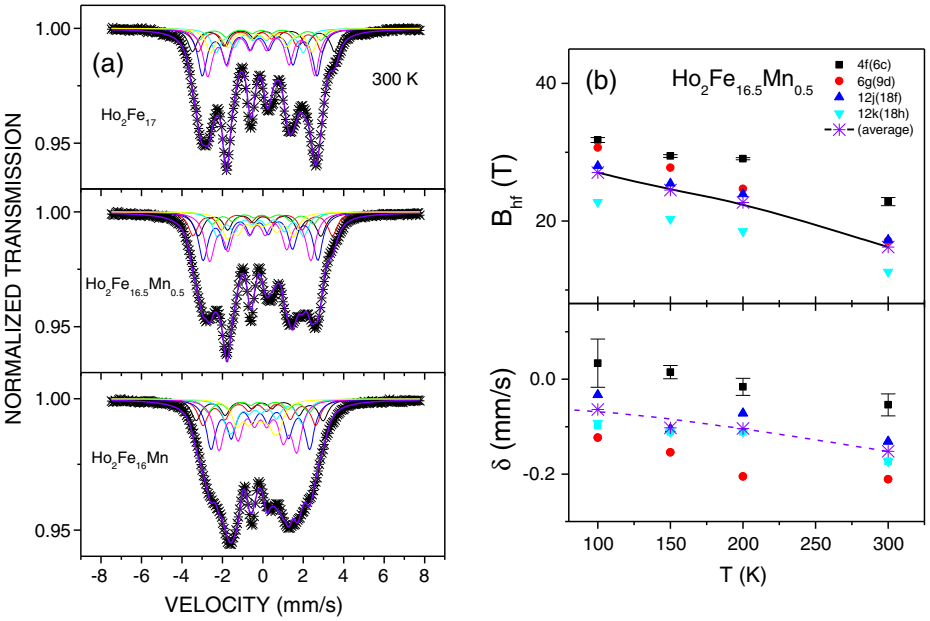

Fig. 1 **a** 300 K Mössbauer spectra of $Ho_2Fe_{17-x}Mn_x$ with x = 0, 0.5 and 1.0. The fits and sub-spectra are described in the text. **b** The temperature dependences of the magnetic hyperfine field and isomer shift values for the various sites of $Ho_2Fe_{16.5}Mn_{0.5}$ with the average values of hyperfine field and isomer shift also shown. The *full line* acts as a guide to the eye for the average hyperfine field values. The *dashed line* represents the second-order Doppler shift calculated with Debye temperature $\theta_D = 450$ K as discussed in the text

Table 1 Mössbauer spectral hyperfine parameters for $Ho_2Fe_{17-x}Mn_x$ at 300 K. The errors for B_{hf} and δ derived from the data fits are ±0.1 T and ±0.015 mm/s respectively

Compounds		4f	6g	12j	12k	Weighted average
Ho_2Fe_{17}	B_{hf}, T	21.9	16.4	18.4	13.6	16.8
	δ, mm/s	0.002	−0.219	−0.111	−0.183	−0.142
$Ho_2Fe_{16.5}Mn_{0.5}$	B_{hf}, T	22.8	17.1	17.3	12.6	16.2
	δ, mm/s	−0.054	−0.211	−0.131	−0.173	−0.152
$Ho_2Fe_{16}Mn$	B_{hf}, T	18.5	15.0	14.4	9.3	13.9
	δ, mm/s	−0.111	−0.23	−0.139	−0.173	−0.147

compounds (see e.g., the similar behaviour of $Ho_2Fe_{17}Mn$ [6]). The isomer shifts are found to behave as $\delta^{4f} > \delta^{12j} > \delta^{12k} > \delta^{6g}$ at all temperatures with the decrease in isomer shift with increasing temperature following behaviour typical of the second-order Doppler shift. The dashed line through the average isomer shift values in Fig. 1b represents the calculated result based on a Debye model [e.g. 9] using Debye temperature $\theta_D = 450$ K.

3.2 Critical magnetic transition

As below, we have carried out a detailed analysis of the magnetisation data around T_C to investigate further the nature of magnetic phase transition in these compounds.

The magnetisation data have been presented elsewhere [6, 7] with the analytical approach following that described in the critical magnetic study of $TbNi_2Mn$ [9].

According to the conventional static scaling law, the critical properties of a second-order magnetic transition can be described by the critical exponents β, γ and δ derived from magnetization measurements around the transition temperature [e.g. 10]. The exponents can be expressed by the following equations:

$$M_S(T) = M_0 \left|(T - T_C)/T_C\right|^{-\beta}, \quad \text{for T} < \text{T}_\text{C} \tag{1}$$

$$\chi_0^{-1}(T) = \left(h_0/M_0\right)\left(T - T_C/T_C\right)^{\gamma}, \quad \text{for T} > \text{T}_\text{C} \tag{2}$$

$$M = DH^{1/\delta}, \quad \text{for T} = \text{T}_\text{C} \tag{3}$$

where M_0, h_0/M_0 and D are the critical amplitudes [10] and M_s and ${\chi_0}^{-1}$ are derived by linear extrapolation from the high-field regions to the intercepts. Using the Kouvel-Fisher method—in which the quantities $M_s(dM_s/dT)^{-1}$ and $\chi_0(d\chi_0/dT)^{-1}$ are plotted against temperature with straight lines of slopes $1/\beta$ and $-1/\gamma$ expected [e.g. 11]—the values of $\beta = 0.45$, $\gamma = 0.95$ and $T_C = 337$ K have been derived for $Ho_2Fe_{16}Mn$ as shown in Fig. 2b. It is clear that the value of T_C derived in this way for $Ho_2Fe_{16}Mn$ is very close to the value $T_C = 338$ K determined from the M-T curves [6, 7]. Indeed this agreement between the T_C values—determined directly from the magnetisation data and derived here from the critical exponent analysis—confirms the applicability of the power laws to these $Ho_2Fe_{17-x}Mn_x$ systems.

Applying (3) to analysis of the critical isotherm at T_C leads to the exponent $\delta = 3.07$ (inset to Fig. 2a). According to statistical theory [10], these critical exponents fulfill the Widom scaling relation: $\delta = 1 + \gamma/\beta$. Using the exponents $\beta = 0.45$ and $\gamma = 0.95$ determined above, the value of δ for $Ho_2Fe_{16}Mn$ is calculated to be $\delta = 3.11$ which is close to the value of $\delta = 3.07$ determined from the critical isotherm analysis at T_C. In a similar manner, the values of β, γ, δ for Ho_2Fe_{17} (of $T_C = 336$ K) and $Ho_2Fe_{15}Mn_2$ (of $T_C = 302$ K) have been determined as $\beta = 0.53$, $\gamma = 0.91$, $\delta = 2.72$ and $\beta = 0.42$, $\gamma = 0.87$ and $\delta = 3.07$, respectively. It is well established that the order parameter of a phase transition around the magnetic transition temperature fluctuates over all available length scales and that these fluctuations smear out the microscopic details of the interactions in a system exhibiting a continuous phase transition [10]. The mean field interaction model for long range ordering has theoretical critical exponents of $\beta = 0.5$, $\gamma = 1.0$ and $\delta = 3.0$, while theoretical values based on the three dimensional Heisenberg model corresponding to short range interactions are $\beta = 0.365$, $\gamma = 1.386$ and $\delta = 4.80$. The β, γ and δ values that we have derived experimentally are generally similar to the mean-field model values, indicating that the ferromagnetic coupling for $Ho_2Fe_{17-x}Mn_x$ compounds is a long-range interaction.

As a further test and cross-check of our critical exponent analyses, Fig. 2c shows the modified Arrot-plots, $M^{1/\beta}$ as a function of $(H/M)^{1/\gamma}$ for $Ho_2Fe_{16}Mn$ using the values of γ and β obtained above. Figure 2c demonstrates clearly that for higher values of the DC fields ($\mu_0 H > 2$ T) these modified Arrot-plots exhibit isothermal curves which are parallel to a high degree (parallel dashed lines are shown as a guide

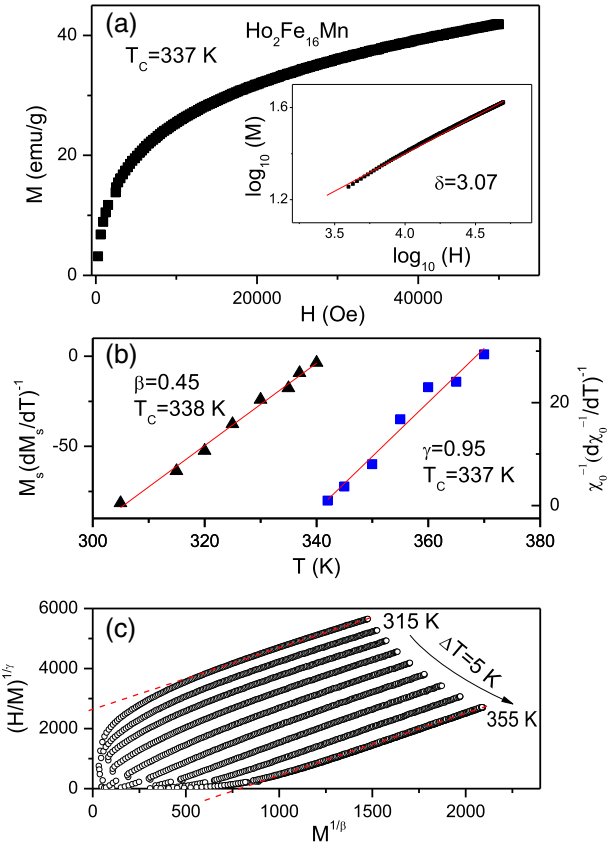

Fig. 2 **a** The critical isotherm analysis at $T_C = 337$ K for $Ho_2Fe_{16}Mn$. The inset shows the data plotted on a double logarithmic scale with the fitted line through the data leading to the exponent $\delta = 3.07$ as described in the text. **b** Kouvel-Fisher plots of $M_s(T)(dM_s/dT)^{-1}$ (*left*) and $\chi_0^{-1}(T)(d\chi_0/dT)^{-1}$ (*right*) versus temperature. The *lines* are fits to the data as described in the text. **c** Modified Arrott plots using $\beta = 0.45$ and $\lambda = 0.95$ as described in the text

to the eye in Fig. 2c) indicating the self consistency of these exponents in describing the critical behaviour of $Ho_2Fe_{16}Mn$.

3.3 Magnetocaloric effect

The isothermal entropy change $-\Delta S_M$ corresponding to a magnetic field change ΔB from B = 0 to value B, has been derived from the magnetization data using the Maxwell relation [e.g. 7]. The changes in magnetic entropy $-\Delta S_M$ for $Ho_2Fe_{16}Mn$ as functions of temperature and external field are shown in Fig. 3a. The curves of $-\Delta S_M$ exhibit a broad peak around T_C (typical behaviour of a second order phase transition) with maximum values of $-\Delta S_M \sim 1.3$ J/kg K and $-\Delta S_M \sim 2.6$ J/kg K for magnetic field changes of $\Delta B = 2$ T and $\Delta B = 5$ T respectively. Mean field theory [12] predicts that $-\Delta S_M{}^{max}$ is proportional to $(B/T_C)^{2/3}$ at second order phase transitions. Figure 3b shows a graph of maximum entropy change $-\Delta S_M{}^{max}$ plotted as a function of $(B/T_C)^{2/3}$ for $Ho_2Fe_{17-x}Mn_x$ with x = 0, 1 and 2. The linear fits to the data in Fig. 3b (fitted curves shown as dashed lines) demonstrate that the relationship $-\Delta S_M{}^{max} \propto (B/T_C)^{2/3}$ is valid for the $Ho_2Fe_{17-x}Mn_x$ system.

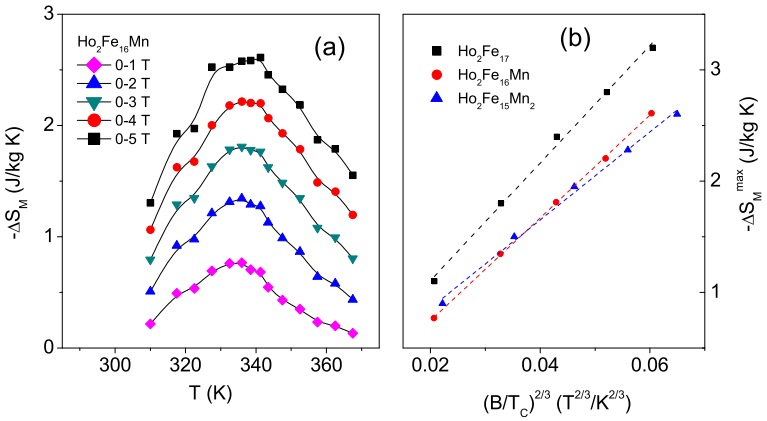

Fig. 3 **a** Temperature dependence of the isothermal magnetic entropy change $-\Delta S_M(T, B)$ as measured in magnetic fields up to 5 T for $Ho_2Fe_{16}Mn$. **b** Dependence of the entropy change $-\Delta S_M{}^{max}$ on the parameter $(B/T_C)^{2/3}$ for $Ho_2Fe_{17-x}Mn_x$ with x = 0, 1 and 2. The *dashed lines* represent linear fits to the data

4 Conclusions

The critical behaviour of $Ho_2Fe_{17-x}Mn_x$ compounds (x = 0–2) has been investigated by combining a Mössbauer spectroscopy study and a detailed analysis of DC magnetization data around their ferromagnetic ordering temperatures of $T_C \sim 340$ K. The four isomer shifts for the four inequivalent sites of their Th_2Ni_{17}-type or Th_2Zn_{17} structures [5] are found to correlate well with the Wigner-Seitz cell volumes as observed previously [6]. The critical exponents determined for $Ho_2Fe_{17-x}Mn_x$ are consistent with the theoretical predictions of the mean-field model, indicating that long range interactions dominate the critical behavior around T_C. The $Ho_2Fe_{17-x}Mn_x$ compounds exhibit reasonable magnetocaloric behaviour as indicated by their isothermal magnetic entropy changes around the Curie temperatures ($T_C = 336$ K, $T_C = 344$ K and $T_C = 338$ K for x = 0, 0.5 and 1.0 respectively), suggesting that these iron-rich alloys allow scope for use as magnetic refrigeration materials close to room temperature.

Acknowledgements This work is supported by a joint agreement between the Australian Nuclear Science and Technology Organisation and the University of Wollongong, and by a grant from the Australian Research Council (DP110102386).

References

1. Brück, E.: J. Phys. D: Appl. Phys. **38**, R381 (2005)
2. Gschneidner, K.A. Jr., Pecharsky, V.K., Tsokol, A.O.: Rep. Prog. Phys. **68**, 1479 (2005)
3. Mandal, K., Yan, A., Kerschl, P., Handstein, A., Gutfleisch, O., Müller, K.H.: J. Phys. D: Appl. Phys. **37**, 2628 (2004)
4. Chen, H.Y., Zhang, Y., Han, J.Z., Du, H.L., Wang, C.S., Yang, Y.C.: J. Magn. Magn. Mater. **320**, 1382 (2008)
5. Wang, J.L., Campbell, S.J., Tegus, O., Marquina, C., Ibarra, M.R.: Phys. Rev. B **75**, 174423 (2007), and reference therein

6. Wang, J.L., Campbell, S.J., Studer, A.J., Kennedy, S.J., Zeng, R.: J. Phys. Conf. Ser. **200**, 082025 (2010)
7. Wang, J.L., Studer, A.J., Kennedy, S.J., Zeng, R., Dou, S.X., Campbell, S.J.: J. Appl. Phys. **111**, 07A911 (2012)
8. Long, G.J., Pringle, O.A., Grandjean, F., Buschow, K.H.J.: J. Appl. Phys. **72**, 4845 (1992)
9. Wang, J.L., Campbell, S.J., Kennedy, S.J., Zeng, R., Dou, S.X., Wu, G.: J. Phys.: Condens. Matter **23**, 2160002 (2011)
10. Fisher, M.E.: Rep. Prog. Phys. **30**, 615 (1967)
11. Freitas, R.S., Haetinger, C., Pureur, P., Alonso, J.A., Ghivelder, L.: arxiv.org/pdf/cond-mat/0010108
12. Oesterreicher, H., Parker, F.T.: J. Appl. Phys. **55**, 4334 (1984)